JOURNAL OF MATERIALS SCIENCE **37** (2002) 4929–4936

The influence of solvent quality on the mechanical properties of thin cast isotactic poly(methyl methacrylate) coatings

B. J. BRISCOE, A. AKRAM
Department of Chemical Engineering, Imperial College, London, SW7 2BY, UK
M. J. ADAMS*, S. A. JOHNSON, D. M. GORMAN
Unilever R&D Port Sunlight, Bebington, Wirral, CH63 3JW, UK
E-mail: michael.adams@unilever.com

Thin coatings of isotactic poly(methyl methacrylate) were cast on glass from solvents of different quality, which was expected to result in different molecular morphologies. The elastic moduli and hardness of the coatings were measured using a nanoindenter. The aim was to examine the viability of this technique for assessing the influence of the morphology on the mechanical properties. The interpretation of the data was complicated by both the influence of the hard substrate and possibly by the plasticising effect of retained solvent in the bulk. Nevertheless, it was reasonable to conclude that a coating cast from a good solvent was stiffer and harder than that from a poor solvent. This is consistent with previous frictional and spectroscopic studies.

1. Introduction

It may be expected that the mechanical and tribological properties of organic polymer coatings will depend on their morphological characteristics since this is the case for bulk specimens. Consequently, there should be a significant influence of the solvent quality on these properties for coatings formed by a solvent casting process. It is well established that the gross mechanical behaviour of polymers in the glassy and semicrystalline states are sensitive to physical ageing during thermal annealing below the glass transition temperature [1]. Solvents also have a marked effect either by acting as a plasticiser or due to solvent induced crystallisation (SINC) [2]. SINC entails the exposure to a solvent of a polymer in the glassy state, which induces crystallisation by increasing the segmental mobility of the chains. This anti-plasticisation process is in addition to other possible microstructural changes such as crazing, shrinkage and the formation of voids. Thus SINC is a different process to crystallisation from dilute solution which is also a relatively well studied process. Much less is known about the morphology and mechanical behaviour of a polymer coating formed by the evaporation of the solvent from what is finally a highly concentrated solution. In the current work, this has been investigated experimentally for isotactic poly(methyl methacrylate) (IPMMA) coatings using nanoindentation in order to measure their elastic moduli and hardness. A potential advantage of this technique is that it is possible to examine very thin coatings, of the order of tens of microns, so that solvent retention is minimised. This is known to be a major problem for organic polymers [3], which can not be avoided by (a) excessive heating because it would result in physical ageing or (b) using ultra thin coatings because the mechanical properties of the supporting substrate would interfere significantly with the response of the indenter when the coating was not sufficiently thick compared with the contact radius. An aim of the preliminary study reported here was to examine the magnitude of these effects in order to establish the viability of the approach. Three solvents were selected from a previous study of the frictional behaviour of coatings prepared from IPMMA [4]. Based on accepted polymer-solvent interactions [5], as characterised by the theta temperature, these solvents were specified as being 'good' or 'poor' (see Table I).

2. Experimental

2.1. Materials and sample preparation

Microscope slides were cleaned in an ultrasonic bath for 1 hr by immersion in dilute aqueous RBS50 solution (Chemical Concentrates (RBS) Ltd., UK). They were then repeatedly rinsed in 'nano-pure' water. IPMMA (Aldrich, Poole, Dorset, UK) was dissolved to a concentration of 1% w/w in chloroform (Aldrich), toluene (BDH, Lutterworth, UK) and carbon tetrachloride (BDH). This could be carried out readily at ambient temperatures for the good solvents but heating to 55°C and mixing with a magnetic stirrer was required for the carbon tetrachloride. The polymer solutions were cast on to the slides using clean dropping pipettes and allowed to dry under ambient conditions for a minimum

*Author to whom all correspondence should be addressed.

TABLE I The average thickness, elastic modulus and hardness at an indentation depth of 100 nm of IPMMA coatings cast from good and poor solvents

Solvent	Solvent quality	Thickness (μm)	Elastic modulus (GPa)	Hardness (GPa)
Chloroform	Good	18	6.5	0.36
Toluene	Good	11	7.2	0.37
Carbon tetrachloride	Poor	34	5.3	0.28

period of 48 hr. In the case of carbon tetrachloride, the slides were initially heated to 60°C in order to prevent quenching of the hot solution. The film thicknesses produced by this method were estimated from the mass per unit area of the dried films (Table I). For comparison purposes, indentation measurements were also carried out on 6 mm thick poly(methyl methacrylate) PMMA sheet (ICI Acrylics).

2.2. Equipment

The mechanical measurements were carried out using a NANO INDENTER®IIs (MTS, Tennessee, USA) which has a theoretical depth resolution of ± 0.04 nm and a load resolution of ± 75 μN, at the low load range employed. It was fitted with a diamond Berkovich probe (triangular based pyramid with an angle of 65.3° between the normal and a face). The tip defect was assumed to have a spherical geometry, and its radius was determined to be *ca*. 50 nm by indenting a silica sample of known elastic modulus and applying Hertz equation [6] to the force-displacement data. The samples were mounted on a computer controlled X-Y micromotion stage that is positioned below an electromagnetically driven indenter assembly. After contact was made between the surface of a coating and the probe tip, a DC current under computer control was applied in order to achieve indentation at a specified velocity to a particular maximum total penetration depth.

An optional continuous stiffness mode is incorporated in the equipment that is based on superimposing an AC current on the DC signal driving the loading ramp [7]. This induces a small probe oscillation, with a peak-to-peak amplitude of 2 nm at a frequency of 45 Hz, during the penetration of a sample. This allows the contact stiffness, S, to be monitored continuously as a function of the measured total penetration depth, h_t, and applied load, W. The contact depth, h_c, may then be determined from the following expression [8]:

$$h_c = h_t - \kappa \frac{W}{S} \tag{1}$$

where κ is a constant equal to 0.75 for a Berkovich probe.

For a perfect conical or pyramidal indenter, the contact area, A, is related to the contact depth, thus

$$A = bh_c^2 \tag{2}$$

where $b = 24.56$ for the Berkovich geometry. Any real indenter has a geometry that deviates from the ideal behaviour. The actual area function of the indenter used here was obtained by a calibration procedure that involved standard silica and aluminium specimens. The results were represented in terms of a polynomial expression of the following form:

$$A = 24.5h_c^2 + \sum_{i=0}^{7} m_i h_c^{1/2^i} \tag{3}$$

where m_i are constants that were evaluated using a curve fitting routine supplied with the equipment.

2.3. Measurement procedure

An indentation test commences with the instrument displacing the probe at a slow velocity of 1 nm/s until there is contact with the surface of the coating as determined by a significant change in the overall system stiffness. From the point of contact, indentation was then carried out at constant velocities of either 1, 5 or 20 nm/s to a maximum depth of 1 μm. The reduced elastic modulus, E^*, of the contact as a function of the total penetration depth was calculated from Equations 1 and 3 using the following expression [8]:

$$E^* = \frac{\sqrt{\pi}\, S}{2\gamma\sqrt{A}} \tag{4}$$

where $\gamma = 1.034$ for a pyramid [8] and

$$E^* = \left[\frac{1-\nu_c^2}{E_c} + \frac{1-\nu_i^2}{E_i}\right]^{-1} \tag{5}$$

such that E is Young's modulus, ν is Poisson's ratio and the subscripts i and c refer to the diamond indenter and the coating respectively. For the purposes of the current work, the mechanical properties of diamond were taken to be $E_i = 1.141$ TPa and $\nu_i = 0.07$, and ν_c was assumed to have the value 0.35. The coating hardness, H, was calculated as follows [6]:

$$H = \frac{W}{A} \tag{6}$$

For the indentation of an isotropic elastic-plastic halfspace with a perfect Berkovich indenter, algebraic manipulation of Equations 1, 2, 4 and 6 shows that the load is expected to increase as the square of the penetration depth provided that the mechanical properties of the material do not exhibit a rate dependence [9]. In this case, the contact depth is also a constant fraction of the total penetration depth, thus [9]

$$\frac{h_c}{h_t} = \frac{1}{1 + \dfrac{\kappa\sqrt{\pi b}}{2\gamma}\left(\dfrac{H}{E^*}\right)} \tag{7}$$

Substitution of Equation 7 into 4 then gives the following linear relationship between the contact stiffness and the total penetration depth for an ideally-shaped probe:

$$S = \frac{2\gamma\sqrt{b}}{\sqrt{\pi}}\left[1 + \frac{\kappa\sqrt{\pi b}}{2\gamma}\left(\frac{H}{E^*}\right)\right]^{-1} E^* h_t \tag{8}$$

The deviations due to rate dependence, the influence of retained solvent and the finite thickness of coatings will be discussed later.

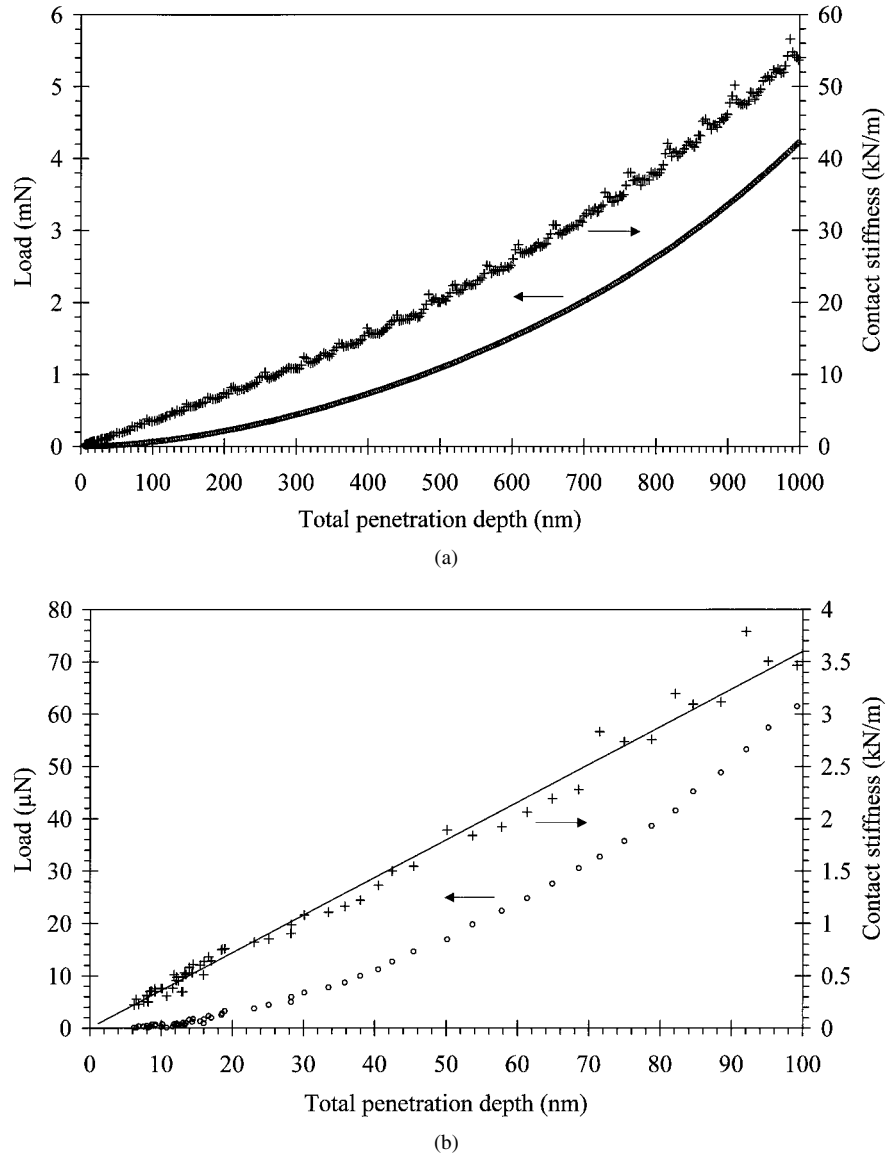

Figure 1 The contact stiffness and load as functions of depth for a chloroform coating corresponding to maximum depths of (a) 1000 nm and (b) 100 nm.

3. Results and discussion

Fig. 1a shows the contact stiffness as a function of the total penetration depth for the coating prepared from the chloroform solution indented at a velocity of 5 nm/s. According to Equation 8, for an elastic-plastic half-space with homogeneous mechanical properties, this plot should be linear which is only the case for about the first 400 nm of penetration. The deviation from linearity at greater depths suggests that a more complex response is involved in this region. Fig. 1b shows more detailed data for the initial 100 nm of indentation; the stiffness data were linear in this region for all the coatings studied. Back extrapolation of the best-fit straight line through the stiffness data can be used to estimate the point at which a perfect Berkovich tip would have contacted the surface. The uncertainty in this contact point determination is about 2 nm, which is the amplitude of the continuous stiffness displacement modulation and approximately the same as the tip defect. The latter is about 3 nm, and represents the vertical height of material 'missing' from a Berkovich probe with a 50 nm radius tip radius.

In Fig. 1b, it can be seen that there are more data points in the region below 20 nm than above, which is a result of the data in this region belonging to the approach segment of the experiment corresponding to a nominal displacement velocity of 1 nm/s. This often occurs when testing compliant materials such as polymers because the system stiffness measurement, which is based on the instantaneous gradient of the static load, is not as sensitive as the dynamic contact stiffness measurement. Consequently, there is some overshoot into the specimen before the 5 nm/s indentation rate is activated. The load as a function of the total penetration depth is also included in Fig. 1 and it may be seen that it provides a considerably less accurate basis for detecting the surface of a specimen.

Fig. 2 shows the load as a function of the total penetration depth for indents carried out at 5 nm/s for coatings prepared from the three solvents. The data represent average values obtained from several indents done under the same conditions although the variability was small (<10%). Corresponding data for a single indentation made in the PMMA sheet are also included in

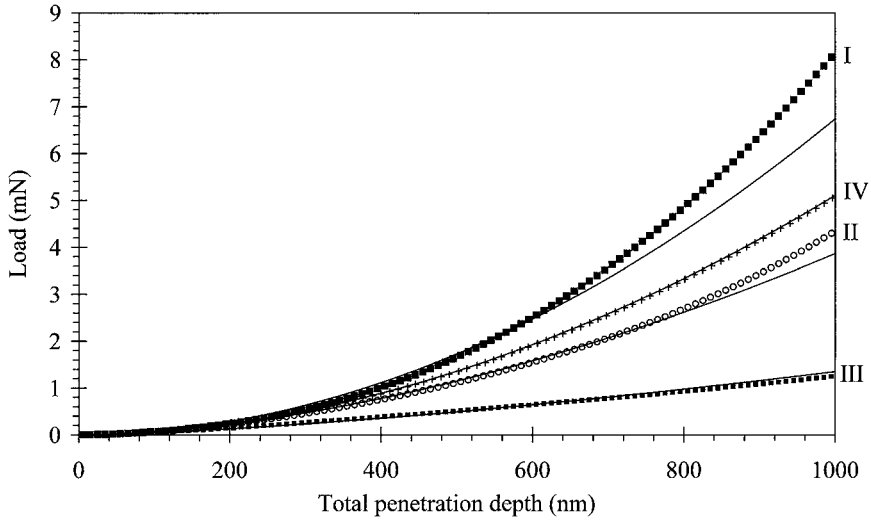

Figure 2 The load as a function of depth at an indentation velocity of 5 nm/s for the toluene (I), chloroform (II) and carbon tetrachloride (III) coatings, and for the PMMA sheet (IV). The coating data are averages obtained for a number of indents, and the curves are the best fits to Equation 9.

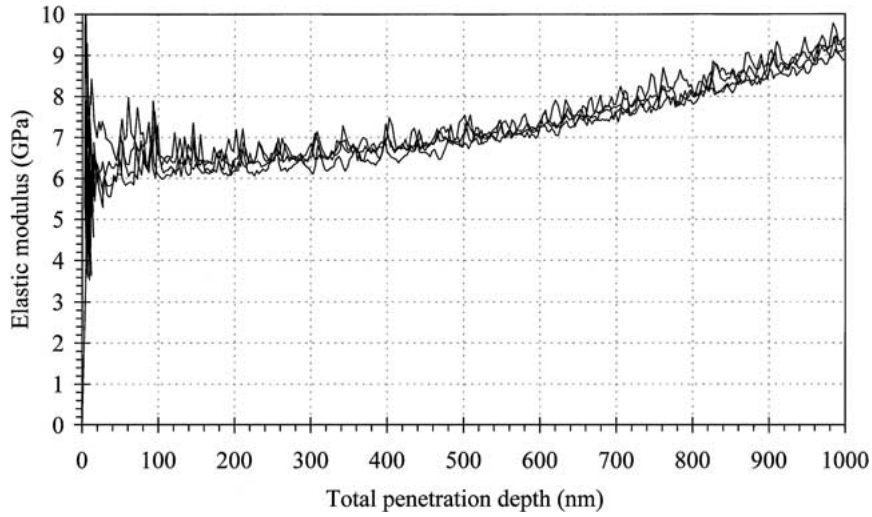

Figure 3 The elastic modulus as a function of depth for four indents carried out at a velocity of 5 nm/s for the chloroform coating.

this figure. They are typical for an isotropic elastic-viscoplastic half-space for which the load is related to the penetration depth as follows [9]:

$$W = b\eta \dot{h}_t^m h_t^{2-m} \tag{9}$$

where $\dot{h}_t$ is the indentation velocity. The parameters η and m are material constants that describe the strain rate dependence of the hardness, thus

$$H = \eta \dot{\varepsilon}^m \tag{10}$$

where the strain rate, $\dot{\varepsilon}$, is given by [10]:

$$\dot{\varepsilon} = \frac{\dot{h}_t}{h_t} \tag{11}$$

The best fits of the data to Equation 9 in the range 5–1000 nm are also included in the figure. In the case of PMMA, the values of η and m are 0.34 and 0.09 which are comparable with the values reported previously; namely 0.37 and 0.07 [9]. The data for the chloroform coating also may be described adequately by Equation 9 except for the positive deviations at depths greater than about 800 nm, which are indicative of the influence of the glass substrate. The value of m for the best-fit line shown is 0.25, which suggests that the strain rate sensitivity is significantly greater than for PMMA. The carbon tetrachloride coating shows near linear behaviour with $m = 0.6$. The best-fit line shown for the toluene coating corresponds to $m = 0.04$ but the fit is inadequate with large positive deviations existing at the greater depths due to the considerable influence of the substrate.

Figs 3 and 4 show four sets of elastic modulus (E_c) and hardness data for a chloroform coating indented at 5 nm/s. In both cases, there is considerable variability in the results for the initial 50 nm. This could be because the coatings were not perfectly smooth which leads to some uncertainty in the contact area at shallow indentation depths. In addition, the indentation velocity in this region is not constant since the indentation velocity in the vicinity of the contact region is of the order of 1 nm/s as described previously. If the hardness is rate dependent then this will also contribute some variability. Consequently, the data in the initial depth region (<50 nm) will not be included in any further figures in order to simplify the interpretation of the data.

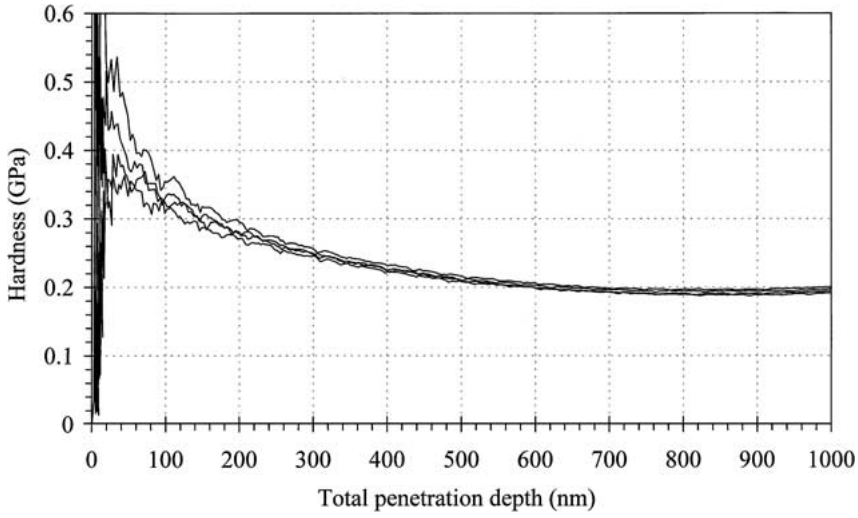

Figure 4 The hardness as a function of depth for four indents carried out at a velocity of 5 nm/s for the chloroform coating.

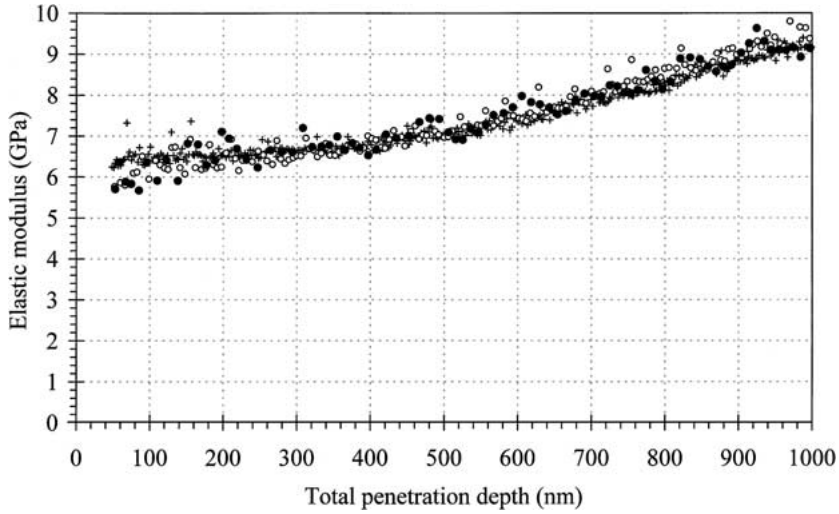

Figure 5 The elastic modulus as a function of depth for the chloroform coating carried out at indentation velocities of 1(+), 5 (○) and 20 (●) nm/s.

Fig. 3 shows that the mean value of the elastic modulus for the chloroform coating is reasonably constant for depths in the range of approximately 50–400 nm. At greater depths, the modulus increases with depth which must arise from the influence of the much stiffer glass microscope slide on which the coating was cast. The hardness of this coating decreases with depth until a minimum value is reached at a depth of about 850 nm (Fig. 4). Such a decrease would occur for any strain rate dependent half-space since the strain rate decreases with depth according to Equation 11. The hardness starts to increase at depths greater than about 850 nm, due to the proximity of the substrate, which is also responsible for the deviation of the power-law fit to the loading curve shown in Fig. 2.

Figs 5 and 6 show single indentation data for the chloroform coating carried out at different velocities. The sensitivity of the hardness data (Fig. 6) to the imposed velocity is a result of the strain rate dependence of the coatings as discussed previously. The data are plotted as a function of the strain rate in Fig. 7 and it may be seen that they superimpose to a good approximation. The best-fit line to Equation 10 of all the data is shown in the figure and the power law parameters are $\eta = 0.56$ GPa.s$^{-0.21}$ and $m = 0.21$. This value for the strain rate dependence of the hardness is similar to that obtained in Fig. 2 ($m = 0.25$) for the power law fit to the average loading curve computed from four indentations done at 5 nm/s. The deviation from the monotonic trend at the lowest strain rates for each data set is due to an increasing contribution associated with the substrate constraint. The superposition of the data in Fig. 7 supports the contention that the initial decrease in hardness with depth for the chloroform-deposited coating may be ascribed to the reduction in strain rate rather than to a gradient in the hardness. The data are less sensitive to the substrate than those for the elastic modulus. This is because the thickness of a coating compared to the contact radius of the indenter has to be much greater for the elastic modulus to be unaffected by the substrate compared with the hardness [11].

The elastic modulus as a function of the indentation depth, at a velocity of 5 nm/s, for the three coatings and the PMMA sheet is shown in Fig. 8. The coating prepared from toluene shows an increase in the values for depths greater than *ca.* 150 nm. The trend is similar to that observed for the chloroform coating except that the increase occurs at a smaller depth; this is because

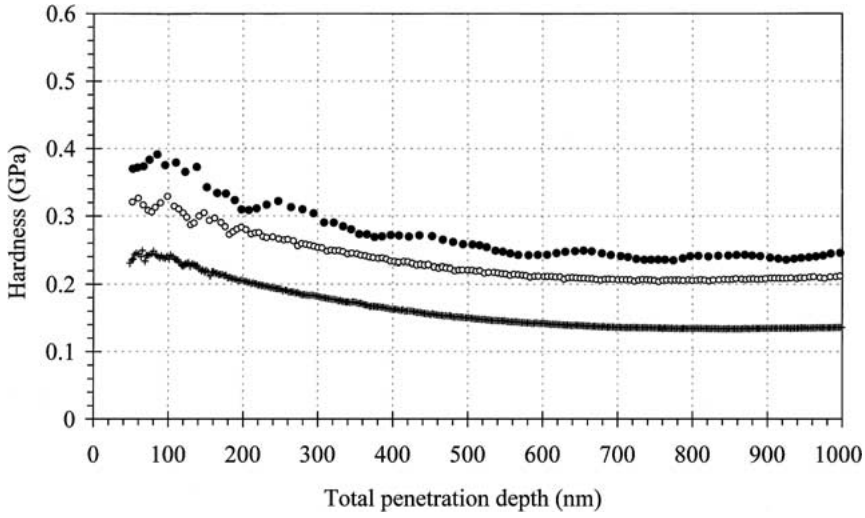

Figure 6 The hardness as a function of depth for the chloroform coating carried out at indentation velocities of 1(+), 5 (○) and 20 (●) nm/s.

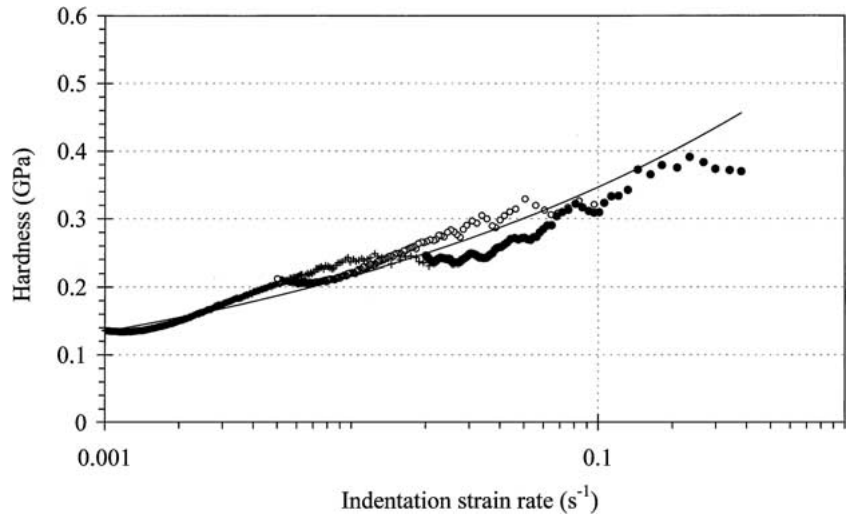

Figure 7 The hardness as a function of strain rate calculated from the data given in Fig. 6.

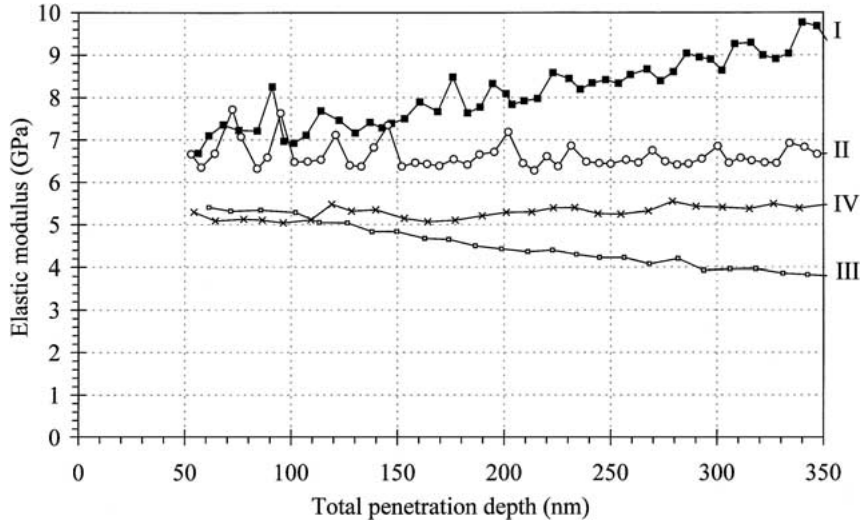

Figure 8 The elastic modulus as a function of the indentation depth, at a velocity of 5 nm/s, for the toluene (I), chloroform (II) and carbon tetrachloride (III) coatings, and for the PMMA sheet (IV).

the thickness of the toluene coating is less. Empirical models have been developed to deconvolute the elastic modulus of a coating from the substrate [12] but they would not be sufficiently accurate for the range of coating thicknesses studied here. In the case of the coating cast from carbon tetrachloride, the elastic modulus is reasonably constant for depths less than *ca.* 100 nm. The values monotonically decrease to a minimum at a depth of about 1000 nm, which suggests that there is a gradient in the mechanical properties. Since the thickness (34 μm) is greater than the coatings formed from the good solvents, it is possible that the softening arises

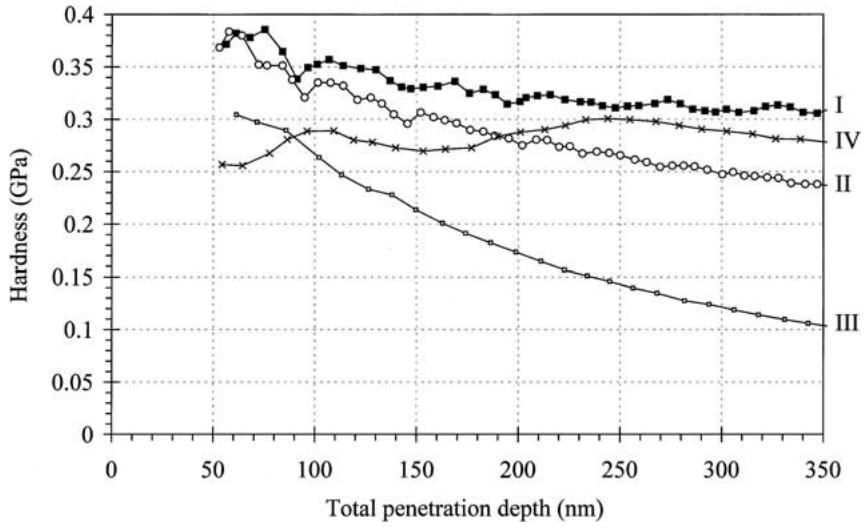

Figure 9 The hardness as a function of the indentation depth, at a velocity of 5 nm/s, for the toluene (I), chloroform (II) and carbon tetrachloride (III) coatings, and for the PMMA sheet (IV).

from the plasticising effect of retained sub-surface solvent. Alternatively, there could be a gradient in the morphology of the coating but independent microstructural measurements would be required in order to examine this possibility.

The hardness data corresponding to Fig. 8 are shown in Fig. 9. The hardness of the toluene coating at depths greater than *ca.* 350 nm, which is not shown in the figure, increases with depth. As in the case of the elastic modulus, this may be attributed to the relative thinness of the coating. Also, as for the behaviour of the elastic modulus, the more rapid decrease in the hardness with depth for the carbon tetrachloride coating compared with that prepared using chloroform may partially arise from retained solvent or a gradient in the morphology. The effect cannot be attributed to strain rate alone because the elastic modulus also decreased in this region and this is measured at a constant strain rate; namely that associated with the amplitude (± 1 nm) and frequency (45 Hz) of the indenter oscillation. Moreover, it was not possible to fit a reasonable strain rate dependence based on the load-depth data (Fig. 2).

In summary, the data are complicated due a gradient in the mechanical properties of the thicker carbon tetrachloride coating and the influence of the glass substrate on the thinner toluene and chloroform coatings. However, it seems reasonable to conclude that, in the region 50–100 nm, the elastic moduli and hardness values as a function of depth are relatively unaffected by these factors. On this basis, the coatings formed from the good solvents are significantly stiffer and harder than those formed from the poor solvent; approximate values of the elastic modulus and hardness in this depth region are given in Table I.

The interfacial shear mechanical properties of various thin solvent cast polymer coatings, including atactic and isotactic forms of poly(methyl methacrylate) have been investigated previously [4, 13]. In these studies, the influence of solvent quality was examined in addition to the effects of subsequent thermal treatments. The interfacial shear strength, τ, was measured using a friction apparatus, which involved sliding a glass hemisphere under a range of normal loads and velocities. It was found that this quantity was linearly related to the contact pressure, p, as follows:

$$\tau = \tau_0 + \alpha p \tag{12}$$

where τ_0 is the intrinsic interfacial shear strength and α is a pressure coefficient; similar behaviour has been found for a wide range of low molecular weight and polymeric thin organic films [14, 15]. The values of α and τ_0 for the cast coatings [4, 13] were found to be greater for the good compared to the poor solvents. Moreover, the parameter α increased with increasing annealing temperature.

The temperature dependence of the interfacial shear strength was examined in the above work [4, 13] for the range 20–160°C. The coatings were characterised as being Type I or II according to the different responses that were observed. Type I behaviour was associated with coatings formed from poor solvents and corresponded to a monotonic decrease in τ, at a specified value of p, as a function of increasing temperature. In the case of Type II behaviour, which was observed for coatings formed from good solvents, τ was constant for temperatures less than that corresponding to the glass transition value, T_g. Further increases in the temperature resulted in a monotonic decrease in τ. Briscoe and Smith [4] applied an Eyring analysis [16] and interpreted these results in terms of the relative crystallinity of the films. It was proposed that good solvents promoted a brittle mode of shear failure, which in gross crystalline systems is known to be relatively independent of temperature. The term 'brittle' was employed to refer to interfacial sliding with limited bulk plastic deformation of the film. The greater pressure coefficients, α, for these systems was thus believed to be indicative of a deforming molecular architecture comprising large moving segments with limited free volume for relative motion. In contrast, poor solvents were considered to produce a more ductile and amorphous microstructure that is sensitive to temperature and shows reduced shear strength.

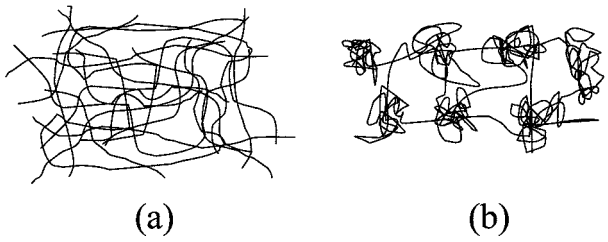

Figure 10 A schematic representation of the molecular architecture produced by (a) good and (b) poor solvents.

An investigation of the structural properties of the above systems using IR spectroscopy was conducted by Briscoe and Thomas [13], which extended the previous work [4] and was generally consistent with the conclusions of their work. They measured the van't Hoff energies from the rate of change of the absorption with temperature and found that this energy for a coating cast from a good solvent was greater than that from a poor solvent. The energies increased with annealing and were greater above the glass transition temperature. The van't Hoff energy is a measure of the molecular mobility arising from rotation about the backbone chain. The molecular architecture developed in the presence of a good solvent is likely to be an extended and interconnected chain network. In the case of a poor solvent, the architecture involves coiled chain domains interconnected by relatively sparsely packed chains. These molecular structures are shown schematically in Fig. 10. It was argued that the uniformly high density of molecular interactions in the extended network accounted for the smaller van't Hoff energy. The more ductile response of the coiled chain structure was thought to arise from the greater conformational mobility in the more sparsely packed regions.

4. Conclusions

Previous frictional and spectroscopic data for coatings of IPMMA cast from solvents of different quality suggest that there should be a difference in the stiffness and ductility depending on the solvent quality. The current data provide direct evidence that this is probably the case. Clearly, further work is required to fully support this conclusion since the interpretation of nanoindentation data obtained from cast thin polymer coatings is complicated by the tip defect, uncertainties in the exact contact point, the influence of the support substrate and possibly by effects resulting from retained solvent or morphological gradients. In the case of coatings thicker than about 20 μm, it would be advisable to examine extended equilibration under vacuum so that the effect of retained solvent can be minimised.

Acknowledgements

We thank EPSRC and Unilever Research for a student bursary (A. A.) and financial support for the nanoindenter.

References

1. M. R. TANT and G. L. WILKES, *Polym. Engng. Sci.* **21** (1981) 874.
2. L. REBENFELD, P. J. MAKAREWICZ, H.-D. WEIGMANN and G. L. WILKES, *J. Macromol. Sci.—Rev. Macromol. Chem.* C **15** (1976) 279.
3. S. BISTAC and J. SCHULTZ, *Prog. Org. Coatings* **31** (1997) 347.
4. B. J. BRISCOE and A. C. SMITH, *J. Appl. Polym. Sci.* **28** (1983) 3827.
5. J. BRANDRUP and E. H. IMMERGUT, in "Polymer Handbook" (Wiley, New York, 1975).
6. K. L. JOHNSON, in "Contact Mechanics" (Cambridge University Press, Cambridge, 1985).
7. W. C. OLIVER and J. B. PETHICA, US Patent no. 4,848,141, July 1989.
8. W. C. OLIVER and G. M. PHARR, *J. Mater. Sci.* **7** (1992) 1564.
9. M. J. ADAMS, D. M. GORMAN and S. A. JOHNSON, *Mat. Res. Soc. Symp. Proc.* **649** (2001) Q7.10.1.
10. B. N. LUCAS and W. C. OLIVER, *Metall. Mater. Trans. A—Phys. Metall. Mater. Sci.* **30** (1999) 610.
11. T. F. PAGE, G. M. PHARR, J. C. HAY, W. C. OLIVER, B. N. LUCAS, E. HERBERT and L. RIESTER, *Mat. Res. Soc. Symp. Proc.* **522** (1998) 53.
12. J. MENCIK, D. MUNZ, E. QUANDT, E. R. WEPPELMANN and M. V. SWAIN, *J. Mater. Res.* **12** (1997) 2475.
13. B. J. BRISCOE and P. S. THOMAS, *STLE Trib. Trans.* **38** (1995) 2382.
14. L. C. TOWLE, *J. Appl. Phys.* **42** (1971) 2368.
15. B. J. BRISCOE and D. TABOR, *J. Adhesion* **9** (1978) 145.
16. S. GLASSTONE, K. J. LAIDLER and H. EYRING, in "The Theory of Rate Processes" (McGraw-Hill, New York, 1941).

Received 30 March
and accepted 21 May 2002